Article

Expansion of Geological CO_2 Storage Capacity in a Closed Aquifer by Simultaneous Brine Production with CO_2 Injection

Seungpil Jung

SK Earthon Co., Ltd., Seoul 03188, Republic of Korea; phil.jung@sk.com; Tel.: +82-2-2121-5114

Abstract: Structural trapping is the primary mechanism for intensive CO_2 sequestration in saline aquifers. This is the foundation for increasing global CO_2 storage; gradual switch to preferable trapping mechanisms, such as residual saturation, dissolution, and mineral trapping, will require a long-time scale. The major constraints limiting the storage capacity of structural trapping are formation pressure and structure size. Over-pressure owing to CO_2 injection causes a disruption of seal integrity indicating a failure in geological sequestration. The other constraint on storage capacity is a spill point determining geological storage volume. Overflowing CO_2, after filling the storage volume, migrates upward along the aquifer geometry with buoyancy. This study proposes a methodology to maximize CO_2 storage capacity of a geological site with a substructure created by an interbedded calcareous layer below spill point. This study provides various conceptual schemes, i.e., no brine production, simultaneous brine production and pre-injection brine production, for geological CO_2 storage. By the comparative analysis, location of brine producer, production rate, and distance between injector and producer are optimized. Therefore, the proposed scheme can enhance CO_2 storage capacity by 68% beyond the pressure and migration limits by steering CO_2 plume and managing formation pressure.

Keywords: pressure-limited capacity; migration-limited capacity; brine production; interbedded impermeable layer; spill point

1. Introduction

Global climate change caused by rapidly increasing greenhouse gas content in the atmosphere poses a great risk to humans. To mitigate this risk, the Paris Climate Change Accord defines the limit of temperature increase to avoid irreversible changes and encourages each member country to meet its own CO_2-reduction targets [1]. For mitigation measures, energy transition from fossil fuels to renewable energy has progressed, but it can only reduce the emission amount of greenhouse gases. Reducing the emission amount alone is not sufficient, and hence, a measure to reduce the overall greenhouse gas content is required. Carbon capture, utilization, and storage (CCUS) is recommended as a key technique that enables the removal of significant amounts of CO_2 from a project perspective.

Aquifers are considered prospective sites for geological sequestration of greenhouse gases. Aquifers containing brine can dissolve CO_2. Particularly, aquifers can sequester CO_2 with high storage efficiency by maintaining the injected CO_2 in a liquid or supercritical phase owing to the hydrostatic pressure and geothermal temperature. However, it has a technical problem of salt precipitation [2], which may clog pore throat resulting in decreasing CO_2 injectivity, and a limitation on the injection volume. The limitation is that the injection volume should not exceed the fracturing pressure of the formation, particularly in a closed aquifer. Injected fluid can induce fractures in formations [3], micro-seismic events [4], and earthquakes [5]. Additionally, a formation pressure higher than the cap rock capillary entry pressure can break the stability of the CO_2 storage system. The fracturing pressure against regional pressurization due to CO_2 injection is a key constraint on the CO_2 storage capacity.

The size of the geological structure is another constraint on the CO_2 storage. The CO_2 storage resource management system (SRMS) highlights a high confidence in the commercial storage of geological formations, as supported by confinement [6]. According to the principle of hydrocarbon fill-and-spill, the remaining CO_2 after displacing the native formation water of the structure migrates upward beyond the spill point. It may be untraceable during the migration along the aquifer; i.e., whether it reaches the biosphere may not be clear. During migration, it can be trapped by residual saturation, mineralization, dissolution, or other structures. However, it can also leak to the surface. The geological structure is the most reliable confinement for geological storage projects. The structure size is generally regarded as pre-determined, but it can be increased if the geological conditions meet specific requirements. Interbedded impermeable layer below the spill point is a potential opportunity for storage capacity expansion. If the injected CO_2 plume is steered to the substructure generated by the cap rock with the interbedded impermeable layer, the storage capacity can be increased without an additional injector.

A traditional strategy is to inject CO_2 and let it flow upwards [7]. Once an injector is drilled in the lower part of the aquifer, CO_2 tends to migrate upward because of its lower density than that of brine. If the upper seal rock functions effectively, injected CO_2 can be trapped in the structure. This concept is applied to depleted oil or gas reservoirs [8], which have a proven sealing structure and reduced formation pressure due to the long period of hydrocarbon production. However, it is challenging to apply this concept to aquifers. The increased aquifer pressure due to the injected CO_2 may result in the mechanical instability of the formation. To mitigate this risk, several concepts of pressure management were suggested in earlier studies [9–13].

Here, an injection scheme with an additional substructure below the spill point is investigated for the structural trap in the aquifer. It applies the strategy of pressure management to prevent the formation of fractures and to steer CO_2 plumes as long as the brine producer does not produce injected CO_2. This study investigates the potential candidate schemes, which are a combination of various types of injectors and producers, from the perspective of quantities of trapped CO_2 in the main structure and substructure, and evolution of the CO_2 plume.

2. Background

2.1. Storage Capacity

Many CO_2 resource management systems were developed for storage estimation, classification, and categorization by various institutes. Most existing storage-resource methodologies approach a volumetric basis [14–17]. It consists of calculating the geological volume in which CO_2 can potentially be stored, and the storage efficiency factor is applied to the calculated volume. The geological storage volume can be calculated numerically using input parameters, despite the inherent uncertainty. The problem is that the storage efficiency factor comprises complicated dynamic factors such as trapping mechanisms, boundary condition, number and type of well, water extraction, and other in situ parameters, which are all related. The volumetric method can only be utilized if sufficient data from regional storage projects are available. Although storage efficiency factors can be revised to reflect pilot tests or actual injection projects, it is technically difficult to evaluate the actual efficiency factor of an individual project. Furthermore, the CCUS industry is still in its initial stage [18–21], and hence, a database for the efficiency factor was never constructed.

The dynamic approach can consider site-specific dynamic factors [22–24]. It simulates the dynamic behavior, which is the result of site operation based on the static model from geological data. The benefits of the dynamic approach are as follows:

- Field specific storage capacity;
- Optimization tool for the development design and operation plan;
- Sensitivity analysis on the uncertainties;
- Fate of CO_2 plume over time.

As with all the simulation methods, it still requires a high cost of computation time and resources and qualified input data for accurate results. However, it is preferable to avoid determining an ambiguous storage efficiency factor.

2.2. Injection Strategy and Pressure Management

The traditional injection scheme involves injecting CO_2 from the lower injector of the aquifer, then let CO_2 upward and trapped by the seal rock [7]. The injected CO_2 is driven to rise through the aquifer due to its lower density than that of the aquifer brine. This results in a larger contact area between the CO_2 and brine with a longer exposure time. Thus, the injected CO_2 plume can be trapped by a stable mechanism such as residual saturation, dissolution, or mineralization. However, the CO_2 quantities trapped by these mechanisms are difficult to measure. Additionally, the remaining mobile CO_2 not trapped by the above mechanisms may migrate outward from the storage site. The structural trap is a reliable storage site to apply the injection scheme of injecting CO_2 from the lower part of the aquifer without migration risk.

However, a structural trap is likely to be a closed system with boundaries by fault, pinch-out, or reservoir heterogeneity. If industrial-scale CO_2 is injected into the compartmentalized formation, it may cause a significant pressure build-up in the aquifer, which can trigger micro-seismic rupture, fault reactivation, and seal fracturing. This can limit the storage capacity of the project. Pressure management by brine production was proposed as a mitigation method. The common advantage of pressure management is that it increases the storage capacity by impeding the pressure build-up to the pressure limit. Additionally, it provides a margin between the actual pressure and estimated pressure limit from a conservative perspective. The methodology is categorized in detail as follows:

- Passive extraction;
- Simultaneous brine production;
- Pre-injection brine production.

The principle of passive extraction is to produce brine from the formation equaling the pressure build-up by CO_2 injection [12]. It exploits the pressure buildup to generate a pressure drawdown of the producer, which is drilled at a location close to the injector. This prevents overpressure near the producer, although its impact on pressure management is limited. The pressure propagates into the entire formation, and therefore, it is not sufficient to relieve the formation pressure by only limiting the pressure drawdown of the producer. Although passive extraction restricts CO_2 breakthrough in the producer, CO_2 breakthrough eventually occurs in the long cycle of the injection operation. This is much worse for pressure management.

Simultaneous brine production [9–11] is an alternative method to passive extraction. The methodology was verified through the industrial-scale project, Gorgon CCS in Australia [25]. As long as the producer is drilled sufficiently far away from the injector, it can produce more brine in a decisive manner with a lower risk of CO_2 breakthrough. However, the brine producer should be drilled in this position for effective pressure propagation for pressure management purposes. However, the efficiency of pressure management has a trade-off with the CO_2 breakthrough. The location of the brine producer should be optimized for each project.

Furthermore, the brine production scheme advances pre-injection brine production [13]. This creates the CO_2 storage site low-pressured zone which provides the same environment as the depleted gas or oil reservoir for the CO_2 storage site. Although it delays the CO_2 injection time in the project life cycle, it is an effective method of pressure management with additional benefits. First, it can reduce drilling costs because the injector can be utilized as a producer prior to injection. It also provides operational benefits such as a smaller area of review (AoR) and less post-injection monitoring. Additionally, through prior brine production as an extended pressure drawdown test, pressure drawdown data can be acquired to estimate the injectivity for actual CO_2 injection. Injection design using injectivity analysis can mitigate the risks of CO_2 injection projects.

In this study, a pressure management scheme for the target storage site is proposed considering the geological and engineering conditions. Several cases representing each injection scheme were applied to the target storage site. By analyzing the pressure behavior and evolution of the CO_2 plume, operational conditions, such as the location of the brine producer and brine production method, were optimized to enhance the CO_2 storage capacity.

3. Evaluation Method

3.1. Geological Description of the Target Aquifer

The target of this study is a hypothetical aquifer, the geological concept of which is based on actual field data. The aquifer was formed between the ancient delta system facies and the uplift carbonate platform facies. The aquifer formation is dominated by marine delta sediments, although there is also a carbonate platform with a stable lateral distribution. As the transgression continued to a late age, carbonate deposition did not occur. The underwater channel and river mouth bar within the delta front facies mainly developed until the seawater reached the carbonate compensation depth. The shore–marine delta deposition system generated thick layers that were stably developed with good lateral continuity. With this geological background, an interbedded calcareous layer can be deposited and a substructure can develop within the main structure. The aquifer structure, including the substructure considered in this study, is illustrated in Figure 1.

3.2. Storage Resources of This Research

This study focuses on the technical storage volume for comparison among storage scheme candidates regardless of project maturity, commerciality, regulations, and other social conditions. The technical storage volume is calculated using dynamic simulations, which can reflect the geological properties and operational conditions of the potential CO_2 sequestration project. To calculate the technical storage volume, the following assumptions on the specific criteria are applied.

3.2.1. Pressure Threshold

A cap rock is the weakest part of geological storage because it is generally more fragile than aquifer formations in terms of lithology [26]. The role of the cap rock is to provide sealing storage so that the injected CO_2 cannot migrate out of the geological storage. Thus, the mechanical stability of the cap is an important aspect of CO_2 geological storage projects. In this study, the upper part of the aquifer formation immediately below the cap rock was considered as a reference point. The fracturing of the cap rock is assumed to occur when the pressure at the point is higher than the fracturing pressure of the cap rock. The fracturing pressure of the cap rock can be estimated by formation leak-off test, destructive testing of the sampled core, mud loss while drilling, or empirical correlations [27]. For this research, the fracturing pressure with depth was estimated by information from offset wells, the seismic velocity, and the empirical correlation [28], which indicated that the fracturing pressure of the cap rock was 27.6 MPa.

For a more reasonable analysis, a geo-mechanical simulation integrated with flow simulation is required. Although the coupled model using the multiphase flow and the geo-mechanical process has been applied to the CO_2 sequestration study [29], several limitations, i.e., instability in low permeability zone and computational bottleneck in industry scaled model were issued [30]. This integrated model cannot guarantee the accuracy of the estimation despite its high computational cost. Considering the estimation uncertainty, 80% of the fracturing pressure of the cap rock was applied as the pressure threshold from a practical perspective. The CO_2 injection duration was from the initial injection to the shut-down point as soon as the local pressure of the reference point reached the pressure threshold for fracturing the cap rock.
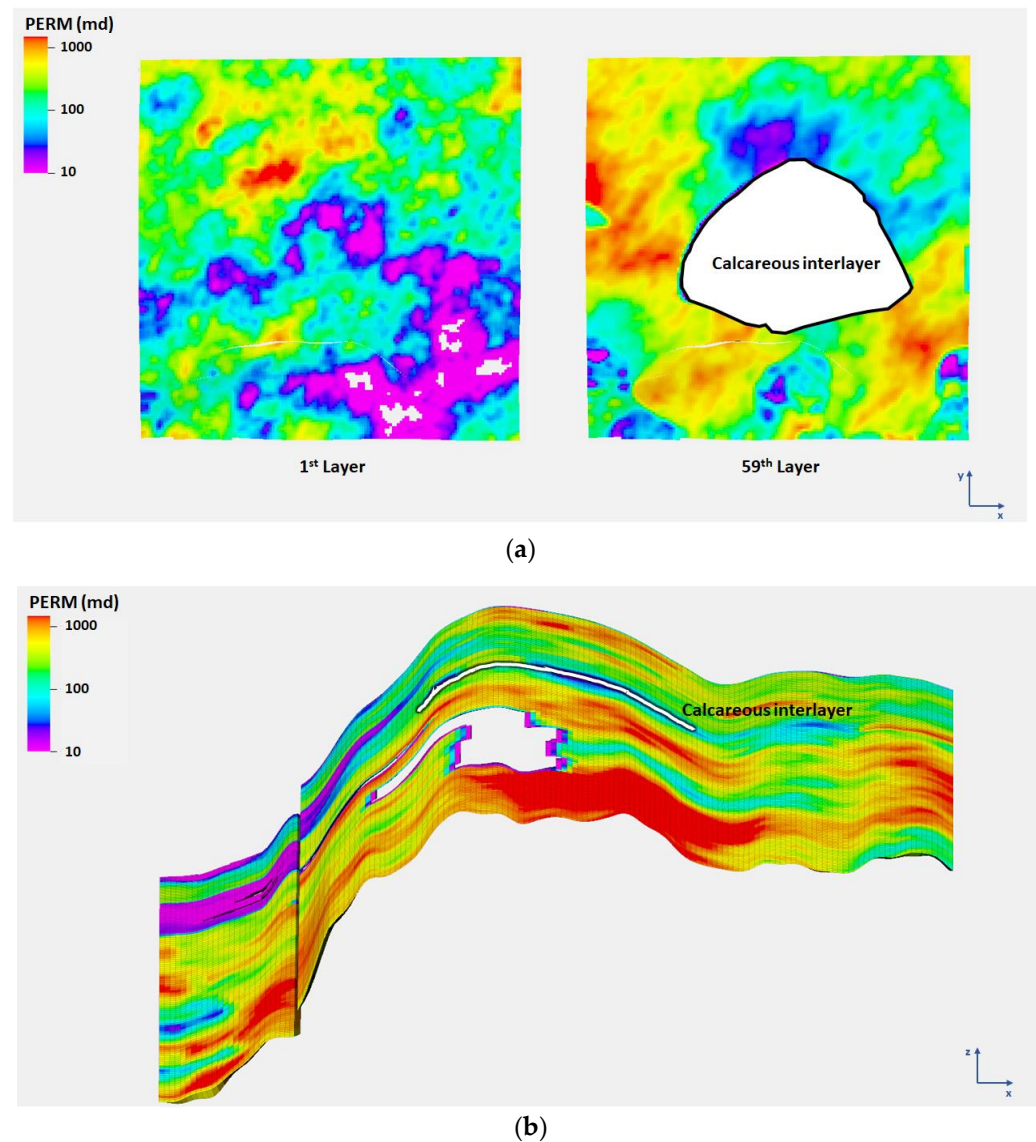
(a)

(b)

Figure 1. Permeability maps depicting the calcareous interlayer which is a cap rock of substructure. (**a**) Planar view (**Left**: top layer, **Right**: 59th layer), (**b**) cross sectional view.

3.2.2. Sequestration Mechanism

The injected CO_2 can be stored in the aquifer through the following four mechanisms:

- Structural and stratigraphic trap;
- Residual saturation trap;
- Dissolution trap;
- Geochemical trap.

Estimates obtained by numerical simulation have a wide range of uncertainty in CO_2 storage capacity, especially for residual traps, solution traps, and mineralization, which are caused by highly uncertain input data for the simulation. These trapping mechanisms categorized into the secondary mechanisms depend on the highly site-specific coefficients and take hundreds of years for the process [20]. The quantity of sequestrated CO_2 is related to the actual cash flow enabled by the government or the trade of carbon credit. From a conservative point of view, the CO_2 quantity in a structure is certified by the storage capacity of the aquifer. The mobile phase and the residual trapped inside the structure were applied as the criteria of a CO_2 storage capacity. For this purpose, the aquifer was categorized into three regions, as shown in Figure 2. Regions 1 and 3 were the main

structures above the spill point and beyond the structure diverging outward, respectively. Region 2 was the other region, including the substructure below the main structure.
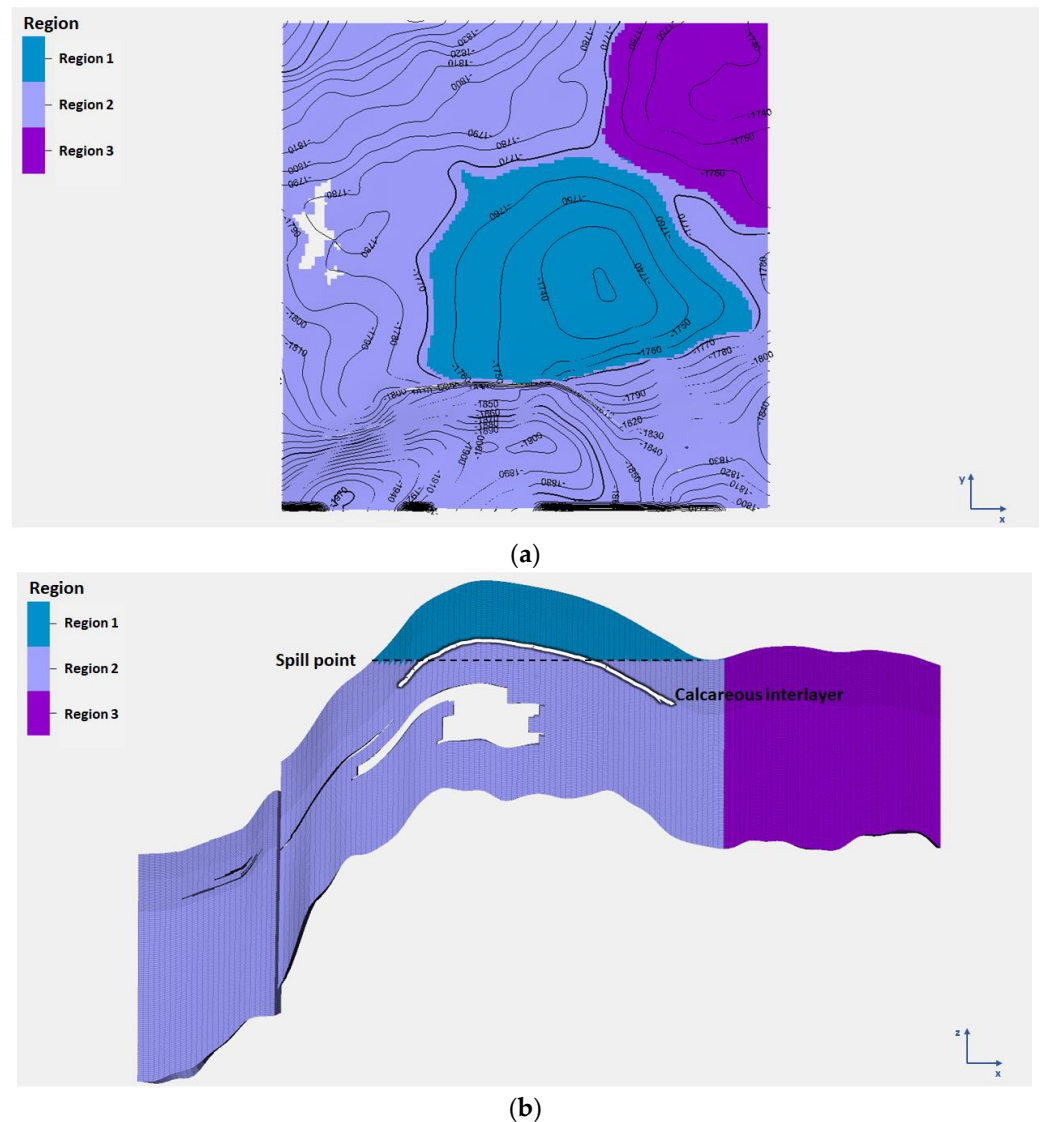

(**a**)

(**b**)

Figure 2. Gradient images illustrating the region classification of the model. (**a**) Planar view, (**b**) cross sectional view.

3.2.3. Timescale

There are two important points in a CO_2 sequestration project: the time of injection cessation and the time of immobilization of free-phase CO_2 [31]. The former is already described in the pressure-threshold section. The injection was stopped as soon as the local formation pressure reached the threshold pressure defined above. The sequestration type of injected CO_2 can be transformed into the above sequestration mechanisms. Generally, while the mobile phase of CO_2 migrates, it is trapped in pore volumes up to the critical saturation or dissolves into the aquifer brine. It can also be mineralized by chemical interactions with specific components of the formation rock. It may have transformed for tens of hundreds of years, but the quantity of transformation decreased after a stabilized CO_2 plume. Through test simulations for the target site, it was confirmed that the transition rate from the mobile phase gradually decreased and the mobile CO_2 plume stabilized approximately 200 years later, as shown in Figure 3. In this research, the storage capacity of CO_2 was determined by the quantity in the structures at 200 years later from commencing injection as the time of immobilization of CO_2.
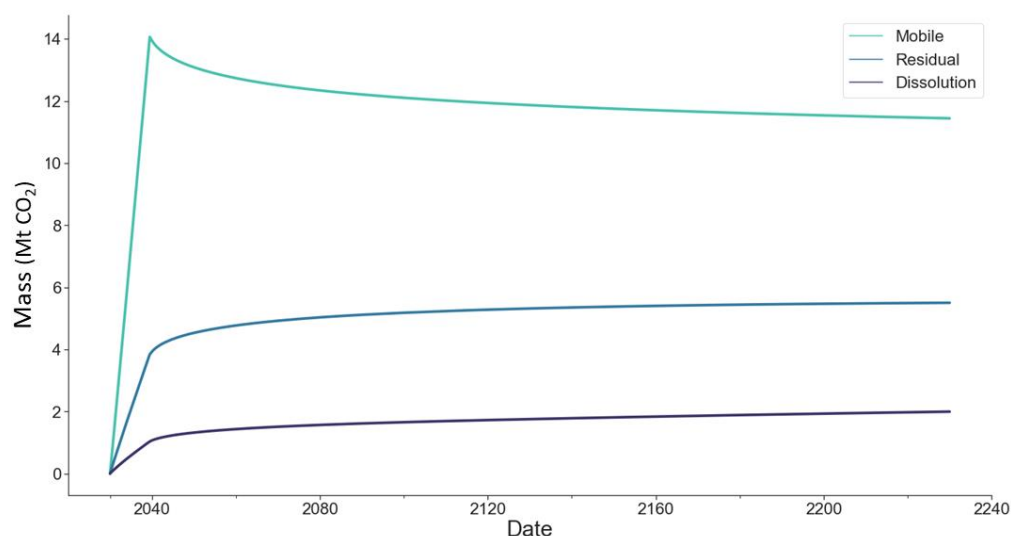
Figure 3. Line graph depicting the temporal evolution of injected CO_2 plume.

Summarily, an accurate quantity of CO_2 sequestration on a reasonable time scale established by the project requires an industrial perspective. It is not only the operational information of a company for ESG management, but also financial information directly related to the commercial activity of the company. If the quantity of CO_2 sequestration is certified as Certificated Emissions Reduction, then it is traded in the carbon credit market, which can be additional earnings for a company. Therefore, the quantity of sequestrated CO_2 should be certified by a strict evaluation method, including monitoring for a sufficiently long period of time. The trapped CO_2 in a structure is more convenient for surveillance than trapped by other mechanisms of residual trapping, dissolution, and mineralization outside of a structure. While these mechanisms relying on parameters with high uncertainty have difficulties in tracking for a sufficiently long time, CO_2 trapped in a structure can be monitored within a limited region with a more confident method. Hence, the quantity of structural and residual saturation trap in a structure is exploited as the main CO_2 storage capacity in this research.

3.3. Model Description

For CO_2 sequestration simulation in a saline aquifer, an isothermal compositional model was utilized [32]. The detailed parameters of the simulation are summarized in Table 1. It is a CO_2-H_2O system in which each component dissolves other components. Sodium chloride, which is the only solid component, determines the salinity of the aquifer. This is a key factor that affects the dissolution of CO_2 in the water phase. As the solid phase is not considered in this study, sodium chloride is assumed to remain in the aqueous phase only.
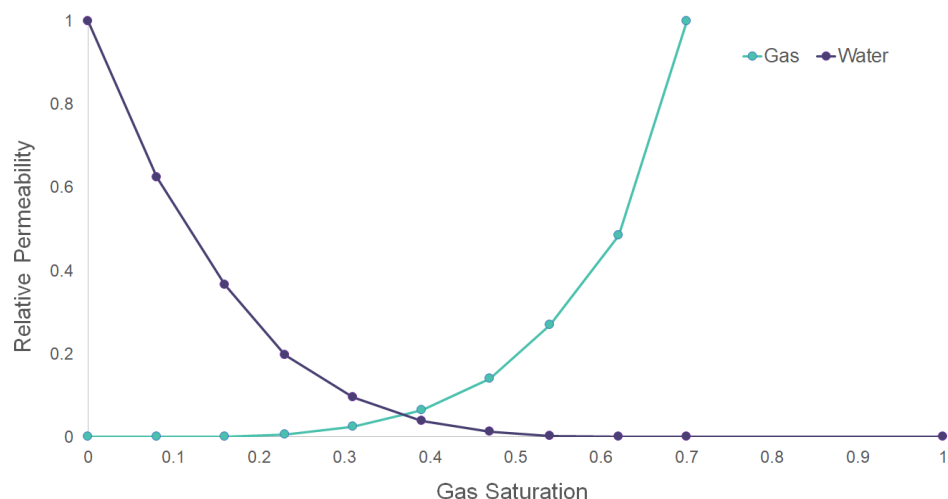
Table 1. Parameters of CO_2 sequestration model.

Phase	CO_2 rich, H_2O rich
Fluid component	CO_2, H_2O, NaCl
Mutual solubility	Phase-partitioning [33]
Molecular diffusion factor	(Unit: m^2/day)
• **Water phase**	H_2O: 0.0005/CO_2: 0.001/NaCl: 0.005
• **Gas phase**	H_2O: 0.001/CO_2: 0.001

A geological model of the potential sequestration site was constructed using the properties summarized in Table 2. The model has 3,232,584 grid blocks covering a 7.5 km by 7.5 km area and 100 m thickness. The relative permeability of CO_2–H_2O system [32] applied to a dynamic simulation is shown in Figure 4.

Table 2. Geological property of aquifer model.

Model dimension (i, j, k)	(152, 153, 139)
Porosity (max, mean, min)	(34%, 24%, 12%)
Permeability (max, mean, min)	(7794 md, 506 md, 3 md)
Vertical/horizontal ratio	0.31
Initial pressure	17.4 MPa @1746 m
Initial temperature	89 °C
Gas residual saturation	30%
Salinity	8%

Figure 4. Line graph of the relative permeability of CO_2-H_2O system.

For computational efficiency, the aquifer model can be extended by attaching an analytic aquifer, which is a widely applied concept in reservoir engineering. The model can be constructed by focusing on the area of review where the injected CO_2 plume migrates or remains. The outside of the model interacts with the numerical model, communicating the pressure by flowing aquifer brine only. The properties of the analytical aquifer are listed in Table 3. The Carter–Tracy aquifer model [34] was adopted as an analytic model, and the influence function assumed that the radius of the analytic aquifer was twice that of the numerical aquifer.

Table 3. Property of analytic aquifer.

Analytic model	Carter–Tracy
Radius numerical aquifer	3800 m
Influence function	2
Permeability	300 md
Porosity	29%

3.4. CO₂ Injection Scenarios

For a comparative analysis of the CO_2 capacity, six scenarios in Table 4 were defined in combination with CO_2 injection and brine production. The first two cases were designed to investigate the effects of the injector location on CO_2 storage. The location of the CO_2 injector is illustrated in Figure 5. The location of the lower injector is below the substructure, which can be filled first with CO_2. The upper injector is located within the main structure immediately below the cap rock. The following four cases were designed to optimize the injection schemes with brine production. CASE 3 applies pre-injection brine production using a single dual-mode well. Brine production and CO_2 injection were performed sequentially in the same well. The last three cases were designed to analyze the effects

of the producer location as shown in Figure 6. The schemes involve CO_2 simultaneous injection with brine production. CASE 4 has a brine producer in opposite direction of the migration pathway. CASE 5 is a revised case of CASE 4 by moving the location of the brine producer close to the migration pathway. The location of the brine producer in CASE 6 is under the crest of the substructure which is sufficient distance apart from the migration pathway. Additionally, the permeability of the completion intervals of CASE 5 and 6 was much higher than that of CASE 4.

The injection condition was to inject CO_2 at a constant rate of 2 Mt/year. When the reference pressure reaches the fracture pressure, CO_2 injection ceases by shut-in. The production condition is a constant rate of production with a lower limit of bottom-hole pressure. The producer was set to produce water at 5000 m^3/day to maintain a bottom-hole pressure higher than 5 MPa. For the cases of simultaneous brine production, brine production stops just before CO_2 reaches the brine producers.

Table 4. Scenario description in combination with CO_2 injection and brine production.

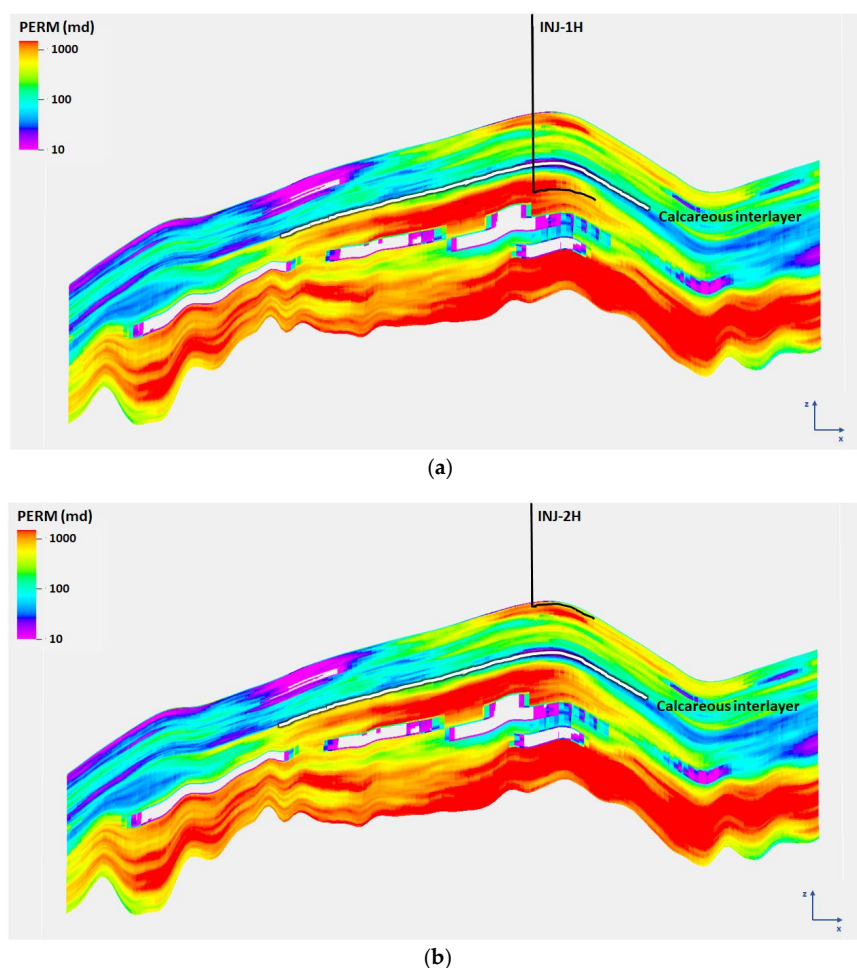| Case	Injector	Producer	Description
CASE 1	Lower	N/A	Injector below substructure
CASE 2	Upper	N/A	Injector right below cap rock of the main structure
CASE 3	Upper	Injector	Pre-injection brine production for 3 years
CASE 4	Upper	Lower	Producer in opposite to the migration direction
CASE 5	Upper	Lower	Producer in the migration pathway
CASE 6	Upper	Lower	Producer away from the migration pathway

(a)

(b)

Figure 5. Permeability maps depicting the location of the injector. (**a**) Lower injector (CASE 1), (**b**) upper injector (CASE 2–CASE 6).
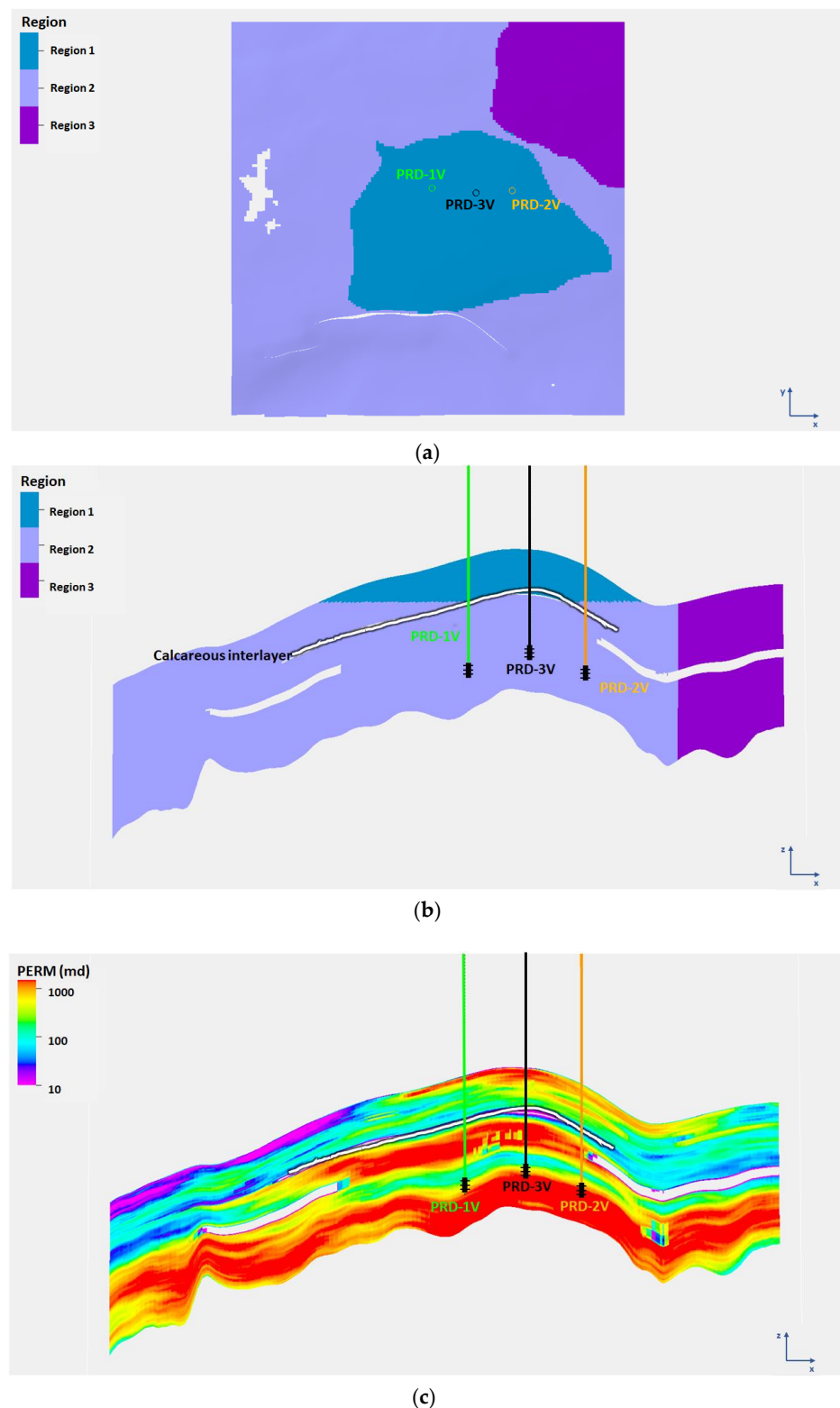
(a)

(b)

(c)

Figure 6. Gradient images showing the location of producer; Producer opposite direction of the migration (PRO-1V for CASE 4), producer close to the migration pathway (PRO-2V for CASE 5), and producer away from the migration pathway (PRO-3V for CASE 6). (**a**) Well location on a planar region map, (**b**) well location on a cross sectional region map, (**c**) well location on a cross sectional permeability map.

4. Results and Discussion

The pressure management strategy was optimized by comparing cases with various combinations of injectors and producers to meet the following requirements. The formation pressure does not exceed the threshold pressure for the fracturing pressure of the cap rock. The injected CO_2 was not produced by brine production. The injected CO_2 can be trapped in the structure as much as possible, particularly in the substructure, by steering the CO_2 plume.

Table 5 summarizes the injection time, total injection mass, and CO_2 capacity, and shows the pressure constraints and effects of pressure management. The lower injector of CASE 1 has a limited effect on the pressure constraint because the injector is located far away from the reference point for the formation fracture, as shown in Figure 5. Additionally, it takes a long time to propagate the pressure buildup from the aquifer bottom due to the calcareous barrier ceiling of the substructure. Additional CO_2 can be injected during the extended time over CASE 2 until the formation pressure reaches the threshold pressure of formation fracture. However, it is the highest limit because the scheme has an obstacle for brine production due to the CO_2 production associated with brine production. The migration direction due to buoyancy is the main reason for not locating the brine producer, even in the upper part of the aquifer. More injection volume without brine production causes the over-pressure around the weak formation, which can be a potential risk on the structure stability.

Table 5. Summary of injection period, injected mass, and storage capacity of CO_2.

Case	Injection Time (year)	Injected Mass (Mt CO_2)	CO_2 Capacity (Mt CO_2)
CASE 1	8.22	16.45	10.13
CASE 2	6.42	12.83	9.79
CASE 3	8.39	16.79	11.87
CASE 4	9.47	18.93	12.92
CASE 5	9.38	18.76	12.77
CASE 6	13.22	26.43	16.44

Pressure management has a significant effect on the CO_2 injection mass summarized in Table 5. It enables at most 6.8 years of additional injection time compared to the cases without brine production. From the formation pressure behaviors shown in Figure 7, the formation pressure of CASE 3, pre-injection brine production, was reduced linearly below the initial formation pressure before ceasing brine production. Then, the formation pressure increased discretely for 3 months, i.e., a shut-in period of 3 months to convert the brine producer into a CO_2 injector. Once CO_2 was injected into the aquifer, the formation pressure increased rapidly until it reached the pressure threshold of the fracturing pressure of the cap rock. The simultaneous brine production case of CASE 4 exhibits a trend of formation pressure increase with a gradual slope. The target production rate is set to 5000 m^3/d, but it cannot meet the target due to the lower limit of bottomhole pressure, as shown in Figure 8. The simultaneous injection with higher rate production in CASE 5 has a dual slope, and its intersection is the point at which brine production stops due to CO_2 breakthrough. Despite the relatively short period of brine production (4.4 years) indicated in Figure 8, a low formation pressure can be maintained due to the higher production rate. Well completion in the interval with higher permeability enables the brine production as much as CASE 4 in a shorter period. CASE 6 shows the longest CO_2 injection time owing to the higher production rate and delayed CO_2 breakthrough. It drives CO_2 injection for 13.2 years, which is longer than that of any other pressure management case.

The injected CO_2 masses categorized by sequestration mechanism and region are summarized in Table 6. The combination of sequestration mechanisms and sequestrated regions can provide a basis for prioritizing the sequestration concept. The sequestration mass by structural traps and residual saturation traps in the main- and the sub-structure

was determined as the CO_2 capacity, as discussed in Section 3.2. The mass beyond the spill point cannot be certified as a proven storage even if it is trapped by saturation residual or dissolution in the simulation results. Although the sequestrated mass by residual and dissolution is known to be stable, the actual quantity is highly uncertain depending on the parameters or coefficients.

Table 6. Classification of sequestrated CO_2 by mechanism and region at year 2230.

	Region	Mobile (Mt CO_2)	Residual (Mt CO_2)	Dissolution (Mt CO_2)
CASE 1	Main structure	3.38	1.51	0.49
	Substructure	5.25	4.14	1.65
	Beyond spill	0.01	0.02	0.01
CASE 2	Main structure	7.37	2.24	0.60
	Substructure	0.18	1.12	0.55
	Beyond spill	0.25	0.36	0.17
CASE 3	Main structure	9.02	2.39	0.60
	Substructure	0.52	1.77	0.83
	Beyond spill	0.65	0.70	0.32
CASE 4	Main structure	9.57	2.37	0.57
	Substructure	0.98	2.27	1.03
	Beyond spill	0.90	0.86	0.40
CASE 5	Main structure	9.47	2.37	0.57
	Substructure	0.93	2.21	1.01
	Beyond spill	0.92	0.88	0.41
CASE 6	Main structure	10.98	2.42	0.54
	Substructure	3.04	3.65	1.52
	Beyond spill	2.17	1.45	0.65

The effects of the injector location were analyzed in two cases, as described in Section 3.3. Only CASE 1 had an injector below the substructure. It fills the substructure first, and then the injected CO_2 migrates to the main structure. Because of the buoyancy of CO_2, its dominant migration direction is vertical. This resulted in a negligibly small mass of migration beyond the spill. While vertically migrating long distances from the aquifer bottom to the top, it sequestrates the large amount of residual trapped CO_2. CASE 1, which sequestrates the most mass in the substructure, contains CO_2 in the main structure as well, as shown in Figure 9a. However, the amount in the main structure is relatively small compared to the whole size of the main structure, and hence, CASE 1 cannot be an efficient sequestration concept. Contrarily, CASE 2 cannot fill the substructure as shown in Figure 9b. The calcareous layer, which is a cap rock of the substructure, acts as a bottom barrier, and buoyancy causes the CO_2 plume to migrate out of the structure.

For the pre-injection brine production in CASE 3, a single well was drilled and utilized as a brine producer and a CO_2 injector sequentially. It is less effective from a pressure management perspective compared to that of CASE 4, 5, or 6 because of the rapid build-up of formation pressure. When shut-in for well conversion, the formation pressure of the reference location recovers immediately. Once the CO_2 injection commences, the recovered formation pressure, which is still below the initial pressure, starts to build up rapidly and finally reaches the pressure threshold of the fracturing pressure, as shown in Figure 7b. As CO_2 is injected into the under-pressured zone by brine production, the scheme displaces the zone with CO_2 rather than overflowing beyond the spill, as shown in Figure 9c. Although it has the disadvantages of project delay and less efficiency, it can be selected for reasons of less CAPEX (capital expenditure) and confident operation based on the test analysis through prior drawdown.
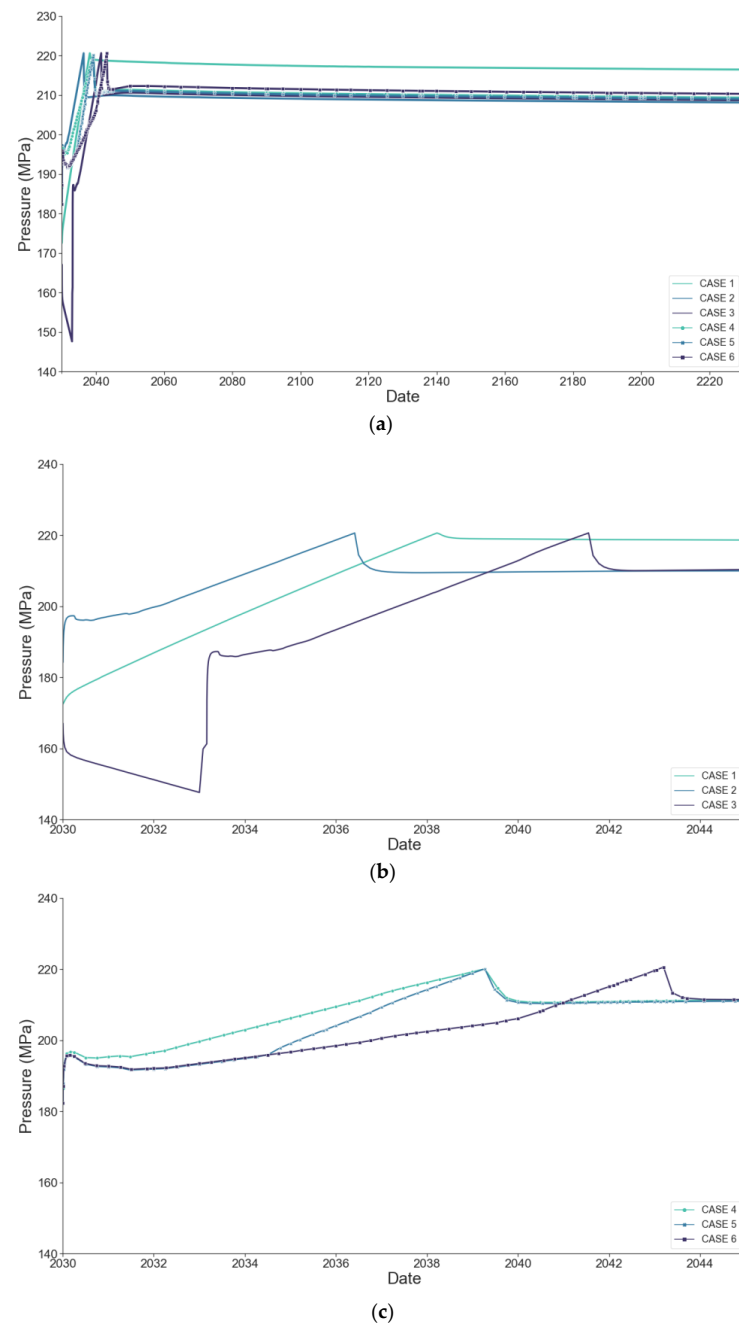
(a)

(b)

(c)

Figure 7. Line graphs showing the comparison of reference pressure below cap rock. (**a**) Pressure behavior for whole 200 years, (**b**) pressure behavior for initial 15 years (CASE1–CASE3), (**c**) pressure behavior for initial 15 years (CASE4–CASE6).

CASE 4 implements pressure management by simultaneous brine production using an additional well. The results show that this is a measure to extend the sequestration capacity by overcoming pressure constraints. It enables an additional 3.1 years of CO_2 injection compared to that of the control case (CASE 2). The additional injection mass was almost 6.1 Mt, although the migration mass beyond the spill increased proportionally to the total injection mass. It still cannot make better use of the substructure for sequestration site considering only 0.98 Mt sequestration mass in the substructure. The brine producer was drilled below the substructure, away from the CO_2 injector, and perforated in the interval with poor permeability. The effects of pressure management were not directly propagated to the reference point of the cap rock. Additionally, the producer is located in the opposite direction to the migration pathway; therefore, there is no drive for the CO_2

plume to dig beneath the cap rock of the substructure. The CO_2 plume from the main structure developed to be distributed both in the substructure and beyond the spill, as shown in Figure 9d.
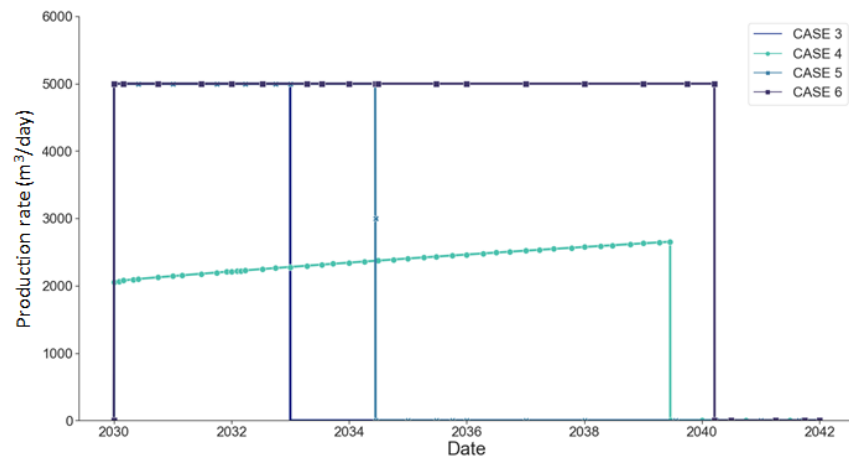

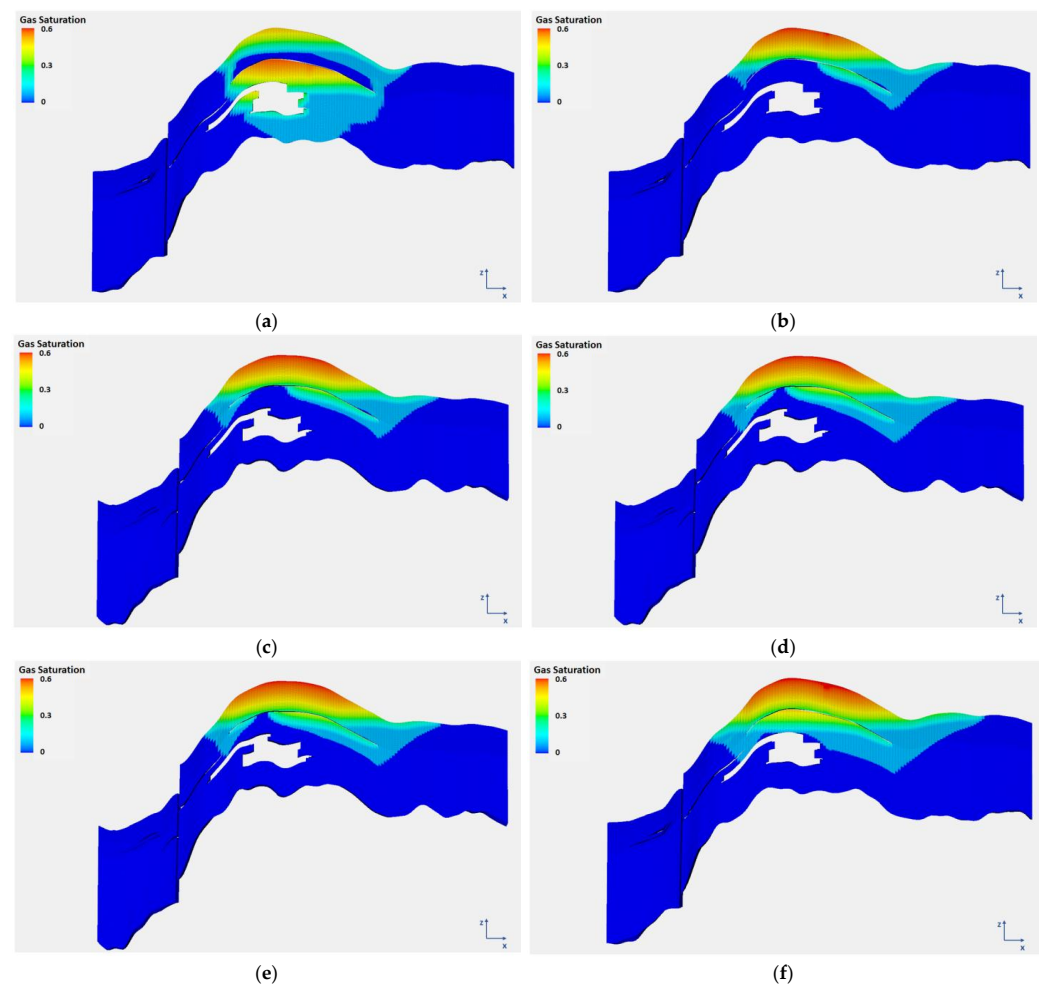**Figure 8.** Line graph depicting the summary of brine production (CASE3–CASE6).

Figure 9. Gradient images depicting the comparison of the distributions of CO_2 at 200 years later from the commencement of CO_2 sequestration project. (**a**) CASE 1, (**b**) CASE 2, (**c**) CASE 3, (**d**) CASE 4, (**e**) CASE 5, (**f**) CASE 6.

CASE 5 has a producer inside the substructure along the migration pathway. The formation pressure was reduced around the brine producer, which drove the CO_2 plume to migrate beneath the top of the substructure. If the brine producer is close to the migration pathway, the steering effects to the substructure can be enhanced, rather than migrating beyond the spill as illustrated in Figure 10. However, early CO_2 breakthrough eventually leads to cessation of CO_2 injection. It acts as another constraint of the CO_2 storage capacity judging from less CO_2 capacity than that of CASE 4.
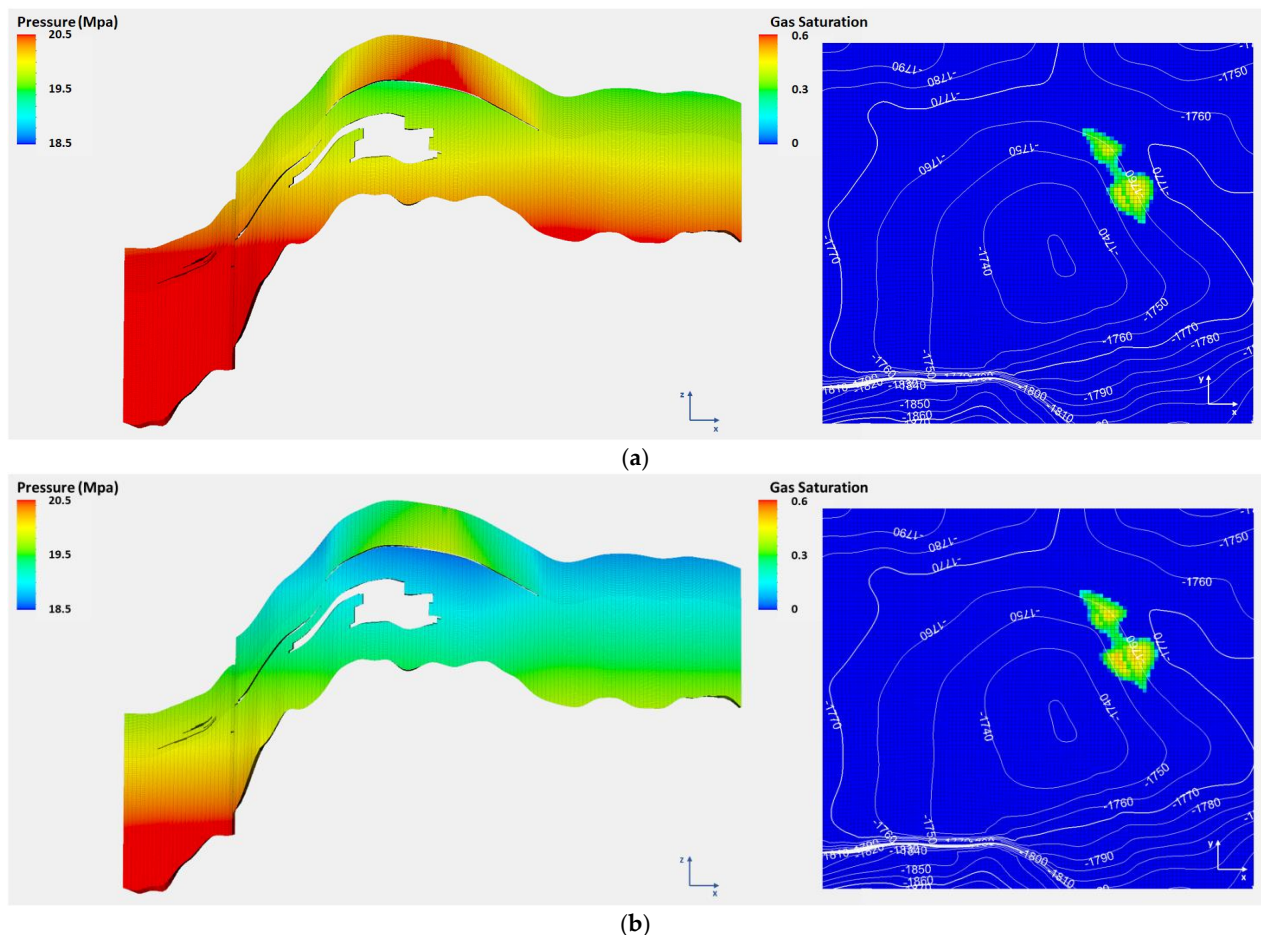

(**a**)

(**b**)

Figure 10. Gradient images showing the behavior of CO_2 plume around the intersection point of the structure outside and the substructure inside. (**a**) Pressure map (cross sectional) and saturation map (planar) of CASE 4 at year 2034, (**b**) pressure map (cross sectional) and saturation map (planar) of CASE 5 at year 2034.

The trade-off between CO_2 steering and pressure management is confirmed through CASE 4 and CASE 5. The key optimization point for maximizing storage capacity is the producer location. Thus, the location of the producer in CASE 6 is moved to the center of the substructure away from the migration pathway. The requirement of the brine producer is to make under-pressured zone near the migration pathway, but sufficient distance away from the migration pathway to delay CO_2 breakthrough. Through the application of this scheme, the substructure accounted for 18% of the total storage capacity. The contribution of the substructure secures an additional 2.1 Mt of CO_2 storage capacity compared to that of CASE 4. The distribution of sequestrated CO_2 plume in the substructure is shown in Figure 9f. The residual trap is depicted in light green color according to the footprint of the CO_2 plume movement. The remaining mobile CO_2 after being trapped by residual saturation is distributed in the top of the substructure with a high concentration of CO_2.

5. Conclusions

Several injection strategies were investigated to overcome the constraints of formation fracture pressure and structure size, which are major constraints that limit the storage capacity in a closed aquifer. The lower injection scheme below substructure showed a good performance only among the cases without pressure management. However, it has no upside potential for the injection period extension because of the systematic limits of CO_2 production associated with brine production. The pressure management with brine extraction was verified as an effective technology from a pressure constraint perspective. It enabled the additional CO_2 injection range from 31% to 106% compared to the cases without pressure management. Focusing on the CO_2 storage capacity, sequestration mass was increased by 6.65 Mt, which is an improvement by 68%. The brine extraction scheme was optimized to maximize the storage capacity by overcoming the constraint of the structure size in the target site, which is part of a closed aquifer with a substructure inside the main structure. Through the optimization, the location of the brine producer was concluded a key parameter for steering the injected CO_2 plume toward the inside of the substructure. For a brine producer, a sufficient distance from the migration pathway and perforation in the high permeability interval have a significant impact on the direction of CO_2 plume movement and evolution.

Conclusively, a CO_2 sequestration strategy to overcome the constraints limiting the CO_2 storage capacity is suggested. Brine extraction extends the CO_2 injection period and evolves the injected CO_2 plume inside the substructure. Through verification of the applicability of brine production, the proposed CO_2 injection scheme can provide key insight into the optimization of a target aquifer considering its geological characteristics. Moreover, the methodology of this study is expected as a practical tool for tacking injected CO_2 plume when combined with the post-injection monitoring data.

Institutional Review Board Statement: Not applicable.

Informed Consent Statement: Not applicable.

Data Availability Statement: Not applicable.

Conflicts of Interest: The author declares no conflict of interest.

References

1. UNFCCC. Paris Agreement. In Proceedings of the Conference of the Parties COP 21, Paris, France, 30 November–12 December 2015.
2. Cui, G.; Hu, Z.; Ning, F.; Jiang, S.; Wang, R. A Review of Salt Precipitation during CO_2 Injection into Saline Aquifers and Its Potential Impact on Carbon Sequestration Projects in China. *Fuel* **2023**, *334*, 126615. [CrossRef]
3. Espinoza, D.N.; Santamarina, J.C. CO_2 breakthrough—Caprock Sealing Efficiency and Integrity for Carbon Geological Storage. *Int. J. Greenh. Gas Control* **2017**, *66*, 218–229. [CrossRef]
4. Goertz-Allmann, B.P.; Kühn, D.; Oye, V.; Bohloli, B.; Aker, E. Combining Microseismic and Geomechanical Observations to Interpret Storage Integrity at the In Salah CCS Site. *Geophys. J. Int.* **2014**, *198*, 447–461. [CrossRef]
5. Ellsworth, W.L.; Giardini, D.; Townend, J.; Ge, S.; Shimamoto, T. Triggering of the Pohang, Korea, Earthquake (M w 5.5) by Enhanced Geothermal System Stimulation. *Seismol. Res. Lett.* **2019**, *90*, 1844–1858. [CrossRef]
6. Frailey, S.; Koperna, G.; Tucker, O. The CO_2 Storage Resources Management System (SRMS): Toward a Common Approach to Classifying, Categorizing, and Quantifying Storage Resources. In Proceedings of the 14th Greenhouse Gas Control Technologies Conference, Melbourne, Australia, 21–26 October 2018.
7. Kumar, A.; Ozah, R.; Noh, M.; Pope, G.A.; Bryant, S.; Sepehrnoori, K.; Lake, L.W. Reservoir Simulation of CO_2 Storage in Deep Saline Aquifers. *SPE J.* **2005**, *10*, 336–348. [CrossRef]

8. Bouquet, S.; Gendrin, A.; Labregere, D.; Le Nir, I.; Dance, T.; Xu, J.; Cinar, Y. CO2CRC Otway Project, Australia: Parameters Influencing Dynamic Modeling of CO2 Injection into a Depleted Gas Reservoir. In Proceedings of the SPE Offshore Europe Oil and Gas Conference and Exhibition, Aberdeen, UK, 8–11 September 2009.

9. Bergmo, P.E.S.; Grimstad, A.-A.; Lindeberg, E. Simultaneous CO_2 Injection and Water Production to Optimise Aquifer Storage Capacity. *Int. J. Greenh. Gas Control* **2011**, *5*, 555–564. [CrossRef]

10. Buscheck, C.A.; Sun, Y.; Chen, M.; Hao, Y.; Wolery, T.J.; Bourcier, W.L.; Court, B.; Celia, M.A.; Friedmann, S.J.; Aines, R.D. Active CO_2 Reservoir Management for Carbon Storage: Analysis of Operational Strategies to Relieve Pressure Buildup and Improve Injectivity. *Int. J. Greenh. Gas Control* **2012**, *6*, 230–245. [CrossRef]

11. Court, B.; Bandilla, K.W.; Celia, M.A.; Buscheck, T.A.; Nordbotten, J.M.; Dobossy, M.; Janzen, A. Initial Evaluation of Advantageous Synergies Associated with Simultaneous Brine Production and CO_2 Geological Sequestration. *Int. J. Greenh. Gas Control* **2012**, *8*, 90–100. [CrossRef]

12. Dempsey, D.; Kelkar, S.; Pawar, R. Passive Injection: A Strategy for Mitigating Reservoir Pressurization, Induced Seismicity and Brine Migration in Geologic CO_2 Storage. *Int. J. Greenh. Gas Control* **2014**, *28*, 96–113. [CrossRef]

13. Buscheck, T.A.; Bielicki, J.M.; White, J.A.; Sun, Y.; Hao, Y.; Bourcier, W.L.; Carroll, S.A.; Aines, R.D. Managing Geologic CO_2 Storage with Pre-injection Brine Production in Tandem Reservoirs. *Energy Procedia* **2017**, *114*, 4757–4764. [CrossRef]

14. Bachu, S.; Bonijoly, D.; Bradshaw, J.; Burress, R.; Christensen, N.; Holloway, S.; Mathiassen, O. *Estimation of CO_2 Storage Capacity in Geological Media*; Carbon Sequestration Leadership Forum (CSLF): Washington, DC, USA, 2007.

15. National Energy Technology Laboratory. *Carbon Sequestration Atlas of the United States and Canada*; US Department of Energy: Washington, DC, USA, 2008.

16. Gorecki, C.; Sorensen, J.; Bremer, J.; Ayash, S.; Knudsen, D.; Holubnyak, Y.; Smith, S.; Steadman, E.; Harju, J. *Development of Storage Coefficients for CO_2 Storage in Deep Saline Formations*; IEA Greenhouse Gas R&D Programme (IEA GHG): Cheltenham, UK, 2009.

17. Brennan, S.T.; Merrill, M.D.; Buursink, M.L.; Warwick, P.D.; Cahan, S.M.; Cook, T.A.; Corum, M.D.; Craddock, W.H.; DeVera, C.A. *National Assessment of Geologic Carbon Dioxide Storage Resources: Methodology Implementation*; Blondes, M.S., Ed.; US Department of the Interior, US Geological Survey: Washington, DC, USA, 2013.

18. Michael, K.; Golab, A.; Shulakova, V.; Ennis-King, J.; Allinson, G.; Sharma, S.; Aiken, T. Geological Storage of CO_2 in Saline Aquifers—A Review of the Experience from Existing Storage Operations. *Int. J. Greenh. Gas Control* **2010**, *4*, 659–667. [CrossRef]

19. Hosa, A.; Esentia, M.; Stewart, J.; Haszeldine, S. Injection of CO_2 into Saline Formations: Benchmarking Worldwide Projects. *Chem. Eng. Res. and Design* **2011**, *89*, 1855–1864. [CrossRef]

20. Kelemen, P.; Benson, S.M.; Pilorgé, H.; Psarras, P.; Wilcox, J. An Overview of the Status and Challenges of CO_2 Storage in Minerals and Geological Formations. *Front. Clim.* **2019**, *1*, 9. [CrossRef]

21. Global CCS Institute. *The Global Status of CCS: 2021*; Global CCS Institute: Melbourne, Australia, 2021.

22. Le Guenan, T.; Rohmer, J. Corrective Measures Based on Pressure Control Strategies for CO_2 Geological Storage in Deep Aquifers. *Int. J. Greenh. Gas Control* **2011**, *5*, 571–578. [CrossRef]

23. Cameron, D.A.; Durlofsky, L.J. Optimization of Well Placement, CO_2 Injection Rates, and Brine Cycling for Geological Carbon Sequestration. *Int. J. Greenh. Gas Control* **2012**, *10*, 100–112. [CrossRef]

24. Gorecki, C.D.; Ayash, S.C.; Liu, G.; Braunberger, J.R.; Dotzenrod, N.W. A Comparison of Volumetric and Dynamic CO_2 Storage Resource and Efficiency in Deep Saline Formations. *Int. J. Greenh. Gas Control* **2015**, *42*, 213–225. [CrossRef]

25. Trupp, M.; Ryan, S.; Mendoza, I.B.; Leon, D.; Scoby-Smith, L. Developing the World's Largest CO_2 Injection System—A History of the Gorgon Carbon Dioxide Injection System. In Proceedings of the 15th Greenhouse Gas Control Technologies Conference, Abu Dhabi, United Arab Emirates, 16 March 2021.

26. Song, J.; Zhang, D. Comprehensive Review of Caprock-sealing Mechanisms for Geologic Carbon Sequestration. *Environ. Sci. Technol.* **2013**, *47*, 9–22. [CrossRef] [PubMed]

27. Zhang, J.; Yin, S.-X. Fracture Gradient Prediction: An Overview and an Improved Method. *Pet. Sci.* **2017**, *14*, 720–730. [CrossRef]

28. Matthews, W.R.; Kelly, J. How To Predict Formation Pressure and Fracture Gradient. *Oil Gas J.* **1967**, *60*, 92–98.

29. Masoudi, R.; Abd Jalil, M.A.; Tan, C.P.; Press, D.; Keller, J.; Anis, L.; Darman, N.; Othman, M. Simulation of Chemical Interaction of Injected CO_2 and Carbonic Acid Based on Laboratory Tests in 3D Coupled Geomechanical Modelling. In Proceedings of the International Petroleum Technology Conference, Beijing, China, 26 March 2013.

30. Gai, X.; Dean, R.H.; Wheeler, M.F.; Liu, R. Coupled Geomechanical and Reservoir Modeling on Parallel Computers. In Proceedings of the SPE Reservoir Simulation Symposium, Houston, TX, USA, 3 February 2003.

31. Bachu, S. Review of CO_2 Storage Efficiency in Deep Saline Aquifers. *Int. J. Greenh. Gas Control* **2015**, *40*, 188–202. [CrossRef]

32. Schlumberger Information Solutions. *Eclipse Technical Description*; Schlumberger: Houston, TX, USA, 2018.

33. Spycher, N.; Pruess, K. A Phase-partitioning Model for CO_2-brine Mixtures at Elevated Temperature and Pressures. *Transp. Porous Media* **2009**, *82*, 173–196. [CrossRef]

34. Carter, R.; Tracy, G. An Improved Method for Calculating Water Influx. *Trans. AIME* **1960**, *219*, 415–417. [CrossRef]